Petroleum Science 23 (2026) 464–474

Contents lists available at ScienceDirect

Petroleum Science

journal homepage: www.keaipublishing.com/en/journals/petroleum-science

Original Paper

CFD study on gas-solid hydrodynamics during the scale-up of high-density circulating fluidized bed

Ming-Zhu Lv [a], Yun-Peng Zhao [a], Min Wang [a,b], Cheng-Xiu Wang [a], Xing-Ying Lan [a], Jin-Sen Gao [a], Xiao-Gang Shi [a,*]

[a] State Key Laboratory of Heavy Oil Processing, China University of Petroleum (Beijing), Beijing, 102249, China
[b] State Power Investment Corporation Hydrogen Energy Co., Ltd, Beijing, 100162, China

ARTICLE INFO

Article history:
Received 13 June 2025
Received in revised form
18 August 2025
Accepted 30 November 2025
Available online 3 December 2025

Edited by Min Li

Keywords:
Scale-up
HDCFB
CFD
Hydrodynamics
Riser height
Riser diameter

ABSTRACT

High-density circulating fluidized bed (HDCFB) offers high gas-solid contact efficiency and shows great application prospects in the petrochemical industry. It is important to study the scale-up of HDCFB for its successful industrial application. Therefore, the gas-solid hydrodynamics of the full-loop HDCFB with different riser heights and riser diameters was systematically investigated by coupling a Euler-Euler model, an energy minimization multi-scale (EMMS) drag model, and a modified solid pressure model. Results demonstrated that the solids circulation rate of the HDCFB system decreases with increasing riser height. When the riser height is 10 m, it is difficult to achieve full development of gas-solid flow. When the riser height increases to 18 m, full development is achieved at a normalized height (h/H) of 0.35. At high solids circulation rates, high riser heights are required to achieve sufficient gas-solid flow development, and adequate storage height is needed to provide the driving force for high-density operation of the circulating fluidized bed. As the riser diameter increases, the pressure drop in each unit of the HDCFB system changes linearly, with the pressure drop in the riser decreasing and the pressure drop in the cyclone separator increasing. In large-diameter risers, the radial distribution of particle concentration and particle velocity inside the riser becomes less uniform, and larger particle clusters can form near the wall with severe particle back-mixing. When the riser diameter increases from 80 to 150 mm, the normalized height of the fully developed gas-solid region increases from 0.15 to 0.42 (h/H), indicating that particles and clusters in large-diameter risers need a longer acceleration zone to develop a stable flow pattern. These findings can provide useful information for the design and scale-up of HDCFB systems.

1. Introduction

The gas-solid circulating fluidized bed (CFB) is widely applied in many industries due to its low energy consumption and capability for continuous operation (Dang et al., 2025; Rodríguez-Machín et al., 2023; Xiong et al., 2020; Yang et al., 2023). Fluid catalytic cracking (FCC) represents its most successful industrial application. With the transformation of the energy structure, the petrochemical industry is shifting from fuel to chemicals. Higher olefin yields are desired in the FCC process, which requires higher solids holdup to enhance gas-solid contact. The HDCFB has great potential for application because of higher concentration and efficient heat transfer. However, most of the studies on HDCFB are experimental and far from the scale of industrial units (Kim et al., 2008; Seo et al., 2012; Wang et al., 2014a). The flow characteristics of HDCFB obtained in experimental units is different from that in industrial units, which makes it difficult to guide flow field regulation within industrial units. Therefore, it is crucial to study the scaling-up law of HDCFB for industrial application and optimization of HDCFB.

Gas-solid CFB can be classified into low-density circulating fluidized bed (LDCFB) and HDCFB based on the differences in solids circulation rate and solids holdup. The LDCFB, such as the CFB boiler, typically has large scale but low solids circulation rate (less than 100 kg/(m^2·s)) and low solids holdup (less than 0.01) (Liu et al., 2010; Lu et al., 2000). The LDCFB has been well-studied in the literature (Luo et al., 2015; Nikolopoulos et al., 2013; Wang

* Corresponding author.
E-mail address: shixiaogang68@cup.edu.cn (X.-G. Shi).
Peer review under the responsibility of China University of Petroleum (Beijing).

https://doi.org/10.1016/j.petsci.2025.11.050

et al., 2017). Tu and Wang (2018) obtained three modes of fluidization at different gas velocities in a CFB with 5.8 m height, finding that particle fluidization is limited by riser height. In contrast, an industrial-scale circulating fluidization boiler with a height of 35 m was simulated by Zhang et al. (2010). The riser is high enough for particles to achieve full development. Noticeable fluctuations in solids holdup occur near the solids recycling inlet. It can be found that the solids circulation rate fluctuates significantly in industrial CFB, which takes longer time for particles to enter the full development region compared to small-scale. The scale-up of the LDCFB has been studied by some scholars. The CFB boilers in lab-scale (0.1 MW), pilot-scale (10 MW), and industrial-scale (100, 300, and 600 MW) were compared by Cui et al. (2021, 2023). The power capacity of the boiler and the coal mass flow rate increase simultaneously during scale-up from lab-scale to industrial-scale. It was found that the particle flow rate and circulating ratio increase with boiler power capacity, significantly enhancing combustion efficiency. Zhu's team compared particle velocities and particle concentrations in risers with heights of 10 m and diameters of 76 and 203 mm, respectively (Yan and Zhu, 2004, 2005; Yan et al., 2005). In the larger-diameter risers, the instability of the gas-solid flow increased, and the radial distribution of particle velocity and particle concentration was steeper, indicating that the riser diameter has a significant effect on the gas-solid flow.

The CFB operating under conditions of solids circulation rate higher than 200 kg/(m^2·s) and solids holdup above 0.1 is defined as HDCFB (Grace et al., 2010). The gas-solid hydrodynamic characteristics in HDCFB are greatly different from LDCFB. Compared to LDCFB, the gas phase carrying capacity of HDCFB is close to its limit. Higher system driving force is required to maintain the pressure balance of the HDCFB system and reduce system fluctuations. The flow characteristics in the HDCFB are more complex due to the higher solids holdup and solids circulation rate. Issangya et al. (1999) built the first cold-flow experimental unit for HDCFB, which consisted of two risers, one riser with a height of 6.1 m and a diameter of 76.2 mm, and the other riser with a height of 9.14 m and a diameter of 101.6 mm. Padssinen et al. and Wang et al. further established an HDCFB with a height of 10 m and obtained gas-solid flow characteristics (Pärssinen and Zhu, 2001; Wang et al., 2014a, 2014b). However, the scale of the experimental unit for HDCFB is extremely different compared to the scale of the industrial unit. It is difficult to build large-scale units in experimental studies, and the computational fluid dynamics (CFD) method has been used by some scholars to study the flow field of the HDCFB. A three-dimensional (3D) full-loop HDCFB with a height of 10 m was simulated by Wang et al. (2011). The axial and radial distributions of solids holdup and particle velocity in the riser are obtained, which are in good agreement with the experiment. Zhang et al. (2015) and Wang et al. (2021), respectively, simulated the 18 m high riser. Zhang et al. focused only on flow characteristics within a single riser, while Wang's two-dimensional simulation lost much comprehensive gas-solid flow information (Zhang et al., 2015). The industrial-scale full-loop HDCFB is rarely reported.

The riser, as a key reaction part in the CFB, is the focus of research (Zheng et al., 2025). Typical risers of laboratory CFB are less than 10 m in height and in the millimeter class in diameter. The risers of industrial CFB are usually over 20 m in height and up to 1 m in diameter (Reh, 1995; Yan and Zhu, 2005; Zhong et al., 2021). Reliable results cannot be obtained from small-scale CFB for industrial design. Therefore, exploring the scaling-up law of HDCFB is necessary. The scale-up process of HDCFB focuses on gas-solid flow, pressure balance, and particle flux within the system. The information provided by single riser simulations is limited, so it is necessary to conduct simulation studies on the full-loop HDCFB. The authors' team has successfully established a pilot-scale HDCFB with 18 m height and achieved stable high-density operation (Su et al., 2019, 2020). Based on the experimental unit, a numerical model of the full-loop HDCFB was further developed to investigate the hydrodynamics within the HDCFB (Wang et al., 2021; Wu et al., 2020). In this paper, the effects of riser height and riser diameter on the gas-solid flow characteristics in the full-loop HDCFB are studied using CFD simulations. A preliminary investigation on the scale-up of HDCFB is conducted, which is helpful for the operation and optimization of industrial units.

2. Methods

2.1. Governing equations

HDCFB is recognized for its high solids circulation rate and strong gas-solid interaction. Accurately describing the flow of the gas and solid phases in an HDCFB is essential to ensure the reliability of numerical simulations. The Euler-Euler model treats both phases as interpenetrating continua, with their motions governed by coupled conservation equations that explicitly account for interphase momentum exchange (Liu et al., 2023). This model offers a balance between computational efficiency and predictive accuracy, which is critical for simulating industrial-scale multiphase systems (Jin and Shen, 2023; Liu et al., 2010). The Euler-Euler model is employed to describe the three-dimensional full-loop gas-solid flow in this work. The capability of this model has been demonstrated in many works, including the author's research team (Wang et al., 2021; Zhang et al., 2023; Zhao et al., 2023). The detailed equations for the Euler-Euler model are presented in Table 1.

In gas-solid flow, the gas-solid drag force plays a decisive role in the particle motion (Kong and Fox, 2017). The formation of particle clusters, which is the common mesoscale structure in HDCFB, significantly reduces the gas-solid drag force. Therefore, the EMMS model considering the mesoscale structure based on the gas-solid nonuniform structure is used. The EMMS is a modification to the traditional drag force model through using a heterogeneity index (H_D), which has been validated in the literature (Guan et al., 2016; Wang et al., 2021; Wu et al., 2016). The solid stress tensor and solid pressure are closed using the kinetic theory of granular flow (KTGF). In the authors' previous work, it was found that the solid pressure of Geldart A particles would be over-predicted when an averaged solid pressure model was used (Wang et al., 2021). Therefore, the solid pressure was corrected by introducing a critical volume fraction of the solid phase ($\varepsilon_{\text{critical}}$) to determine the different contributions of clusters in the dilute and dense phase regions. The critical value for solids holdup is set at 0.1 based on the definitions of LDCFB ($\varepsilon \leq 0.1$) and HDCFB ($\varepsilon > 0.1$) (Bi and Zhu, 1993). The correction for the solid pressure is shown in the following equation, which was described in detail in the authors' previous work (Wang et al., 2021).

$$p_s = \begin{cases} 0.05 \times p_{s,0}, & \varepsilon_{\text{critical}} > 0.1 \\ 0.3 \times p_{s,0}, & \varepsilon_{\text{critical}} \leq 0.1 \end{cases} \quad (1)$$

2.2. Simulation object

The experimental setup of HDCFB developed in the authors' group was used as the simulation object in this paper, as shown in Fig. 1. The HDCFB consists of a riser, a cyclone separator, a downcomer, a storage tank and a feed pipe. The riser is 18 m high with a diameter of 80 mm, the downcomer is 8 m high with a diameter of

Table 1
Governing equations of the Euler-Euler model.

Continuity equation:
$\frac{\partial}{\partial t}(\varepsilon_m\rho_m)+\nabla\cdot(\varepsilon_m\rho_m u_m)=0$
Momentum equation:
$\frac{\partial}{\partial t}(\varepsilon_m\rho_m u_m)+\nabla\cdot(\varepsilon_m\rho_m u_m u_m)=-\varepsilon_m\nabla\cdot p+\nabla\cdot\tau_m+\varepsilon_m\rho_m g-\beta U_{s,g}$
Granular energy equation:
$0=(-p_s\boldsymbol{I}+\tau_s):\nabla\boldsymbol{u}_s-\gamma_s-3\beta\Theta_s$
Constitutive equations:
Stress tensors:
$\tau_g=\varepsilon_g\mu_g[\nabla\boldsymbol{u}_g+(\nabla\boldsymbol{u}_g)^T]-\frac{2}{3}\varepsilon_g\mu_g\nabla\cdot\boldsymbol{u}_g\boldsymbol{I}$
$\tau_s=\varepsilon_s\mu_s[\nabla\boldsymbol{u}_s+(\nabla\boldsymbol{u}_s)^T]+\varepsilon_s\left(\lambda_s-\frac{2}{3}\mu_s\right)\nabla\cdot\boldsymbol{u}_s\boldsymbol{I}$
Solid phase pressure:
$p_{s,0}=\varepsilon_s\rho_s\Theta_s+2\rho_s(1+e_s)\varepsilon_s{}^2g_0\Theta_s$
Solid phase shear viscosity:
$\mu_s=\mu_{s,kin}+\mu_{s,col}+\mu_{s,fr}$
Bulk viscosity:
$\lambda_g=0$
$\lambda_s=\frac{3}{4}\varepsilon_s\rho_s d_p g_0(1+e_s)\left(\frac{\Theta_s}{\pi}\right)^{1/2}$
Radial distribution function:
$g_0=\left[1-(\varepsilon_s/\varepsilon_{s,max})^{1/3}\right]^{-1}$
Diffusion coefficient for granular energy:
$\kappa_s=\frac{150\rho_s d_p\sqrt{\Theta_s/\pi}}{384(1+e_s)g_0}\left[1+\frac{6}{5}g_0\varepsilon_s(1+e_s)\right]^2+2\rho_s\varepsilon_s^2 d_p(1+e_s)g_0\sqrt{\Theta_s/\pi}$
Collisional dissipation of energy:
$\gamma_s=\frac{12(1-e_s^2)\varepsilon_s^2\rho_s g_0\Theta_s^{3/2}}{d_p\sqrt{\pi}}$

450 mm, and the storage tank is 6 m high with a diameter of 660 mm. The gas phase enters the system through the bottom of the riser, and the particles enter the riser from the storage tank via the feed pipe. Mixing of the gas and solid phases occurs at the bottom of the riser. At the top of the HDCFB, the gas-solid phases are separated by the cyclone separator, where the gas phase leaves the HDCFB and the solid phase returns to the downcomer and storage tank to complete the circulation. To maintain a constant particle volume, particles discharged from the top of the cyclone separator were returned to the storage tank using a user defined function (UDF). A small amount of fluidized air is added at the bottom of the storage tank to maintain normal particle fluidization in the full-loop HDCFB.

2.3. Simulation system and setup

In the simulation of a full-loop HDCFB, air is regarded as the gas phase and typical FCC industrial catalyst is regarded as the solid phase. The physical properties of the gas and solid phases are provided in Table 2. The inlet boundary condition is set as velocity-inlet. At the top of the cyclone separator, atmospheric pressure is used as the outlet boundary condition. The no-slip boundary condition is used at the wall.

The HDCFB geometry was divided into hexahedral cells in ANSYS Icem, with a total cell count of 300,000. The commercial software ANSYS Fluent was used as a solver to solve the transient equations. Pressure-velocity was coupled by the SIMPLE method. The momentum and energy equations were discretized using the second-order upwind scheme, with a residual convergence criterion of 10^{-5}. The HDCFB simulations under different operating conditions were performed with a time step of 0.0005 s for a total of 40 s to achieve a steady-state flow field. Time-averaged results were obtained from 40 to 60 s.

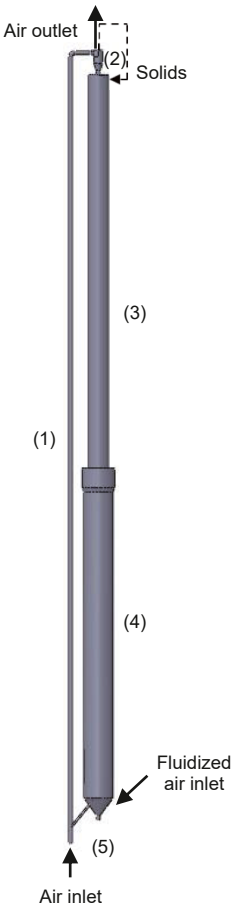

Fig. 1. Structure of the HDCFB: (1) riser, (2) cyclone separator, (3) downcomer, (4) storage tank, (5) feed pipe.

3. Results and discussion

3.1. Model validation

Typical high-density operating conditions in the experimental setup were selected for model verification. In the full-loop CFB simulation, the gas velocity at the bottom of the riser was 7 m/s, the particle packing height in the storage tank (storage height) was 6 m, and the fluidized air flow rate at the bottom of the storage tank was 12 m^3/s, which was consistent with the experimental setup operation. To verify the accuracy of the full-loop HDCFB model developed in this paper, simulation results were compared with experimental data, as shown in Fig. 2. The results show that the axial and radial distribution of solids holdup in the riser are in good agreement with the experiment. The solids holdup is relatively high at the bottom of the riser and gradually decreases with increasing riser height. The axial distribution trend of solids holdup is consistent with the experimental data. In the radial direction of the riser, the distribution of solids holdup is higher near the wall and lower in the center, showing a typical “core-annular” flow structure. As the axial height increases, the radial distribution of solids holdup becomes more uniform. The time-averaged solids circulation rate obtained from the full-loop HDCFB simulation is 630 kg/(m^2·s), which is close to the 650 kg/(m^2·s) measured in the experimental setup. The pressure drop in the riser of the full-loop HDCFB is 45.8 kPa, with a relative error of 6.5% compared to the 43 kPa pressure drop observed in the experiment. Therefore, the HDCFB model developed in this paper is reliable for describing the hydrodynamics in the actual experimental setup.

Table 2
Properties of gas phase and solid phase.

Items	Values
Air density, kg/m^3	1.225
Air viscosity, Pa·s	1.7894×10^{-5}
Particle density, kg/m^3	1500
Particle diameter, m	8.5×10^{-5}

3.2. Effect of riser height on gas-solid hydrodynamics in the HDCFB

For the riser reactor, the height and diameter are key structural parameters that significantly influence gas-solid flow. The height of the riser can influence both the inlet region and the flow development. Therefore, it is necessary to investigate the impact of riser height on gas-solid flow within the HDCFB.

The HDCFB geometries of different riser heights are built, as shown in Fig. 3. The operating conditions are shown in Table 3, where the size of the storage tank is kept constant to ensure consistent driving force in the different structures.

Table 4 summarizes the pressure distribution of the HDCFB. The pressure balance within the HDCFB is crucial for the stable operation of the high-density system. It is essential to maintain a well-regulated pressure loop to ensure stable hydrodynamics of the particles within the HDCFB. In the CFB system, the driving force comes from the cumulative hydrodynamic pressure drop across three key components: the storage tank, the feed pipe, and the downcomer. The storage tank provides most of the pressure drop due to the high storage height in the storage tank. The feed pipe contributes a smaller pressure drop, mainly caused by the static pressure of the particles. The downcomer has almost no pressure drop because particles fall freely. The resistance in a CFB system primarily comes from the pressure drop across the riser and the cyclone separator, which comprise contributions from static pressure, friction losses, etc. The pressure balance of the HDCFB system is obtained from the following equation:

$$\Delta P_{ds} + \Delta P_{fp} = \Delta P_{riser} + \Delta P_{cyc} \quad (2)$$

where ΔP_{ds} is the pressure drop of the storage tank and downcomer, ΔP_{fp} is the pressure drop of the feed pipe, and ΔP_{riser} is the pressure drop of the riser, including the static pressure of the gas phase and solid phase, the acceleration of the particles and the friction between the gas phase, solid phase and the wall. ΔP_{cyc} is the pressure drop of the cyclone separator.

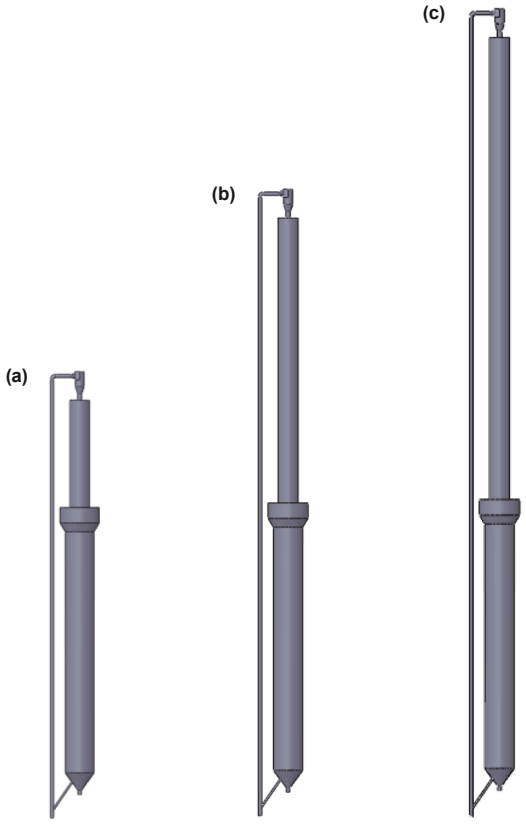

Fig. 3. Geometry of HDCFB with different riser heights. **(a)** $H_r = 10$ m, **(b)** $H_r = 14$ m, **(c)** $H_r = 18$ m.

Table 4 shows that the difference in pressure drop distribution within the HDCFB of different riser heights is very small. This result indicates that when the catalyst loading is kept constant, the pressure drop in each unit is basically constant for the HDCFB of different riser heights. The variation of solids circulation rate over time in the gas-solid HDCFB of different riser heights is shown in Fig. 4. As the height of the riser increases, the solids circulation rate of HDCFB

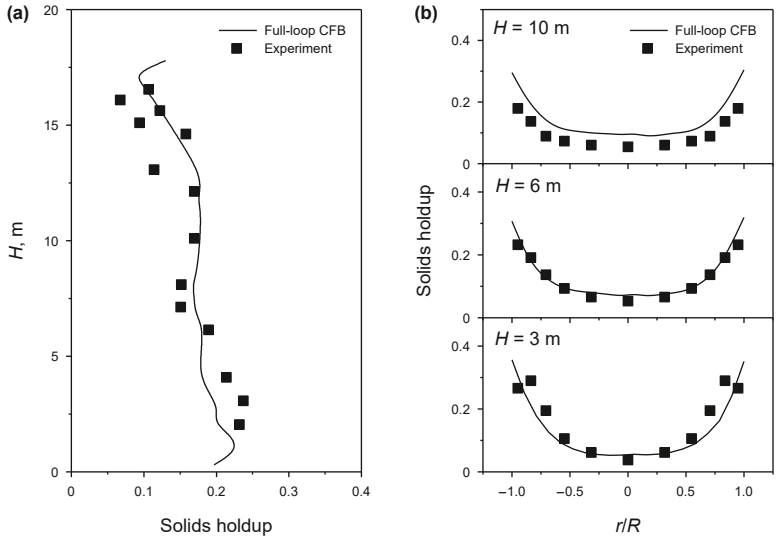

Fig. 2. Comparison of solids holdup in the riser between simulation and experiment. **(a)** Axial solids holdup, **(b)** radial solids holdup.

Table 3
Operating conditions of HDCFB with different riser heights.

Items	Values
Riser height, m	10, 14, 18
Riser diameter, mm	80
Superficial gas velocity, m/s	5
Storage height, m	6
Fluidized air, m^3/h	12

Table 4
Pressure distribution of HDCFB with different riser heights.

Pressure drop, kPa	$H_r = 10$ m	$H_r = 14$ m	$H_r = 18$ m
ΔP_{riser}	51.07	51.05	50.59
ΔP_{cyc}	0.12	0.10	0.05
ΔP_{fp}	−0.86	−0.91	−0.92
ΔP_{ds}	−50.33	−50.24	−49.72

In the table, positive values indicate resistance and negative values indicate driving force.

decreases significantly. This result is due to the fact that the solids circulation rate within the HDCFB is influenced by the pressure drop distribution. Particle static pressure is a major component of the pressure drop in the riser and is mainly affected by particle concentration and reactor height. Higher solids circulation rates and higher riser heights result in higher static pressures. Therefore, a high solids circulation rate can be achieved with a lower riser when the system driving force is constant. As the riser height increases, the driving force provided by the HDCFB system is insufficient to maintain a high solids circulation rate due to the constant storage height. In order to achieve full-loop flow of solids within the CFB, the solids circulation rate in the riser will decrease. For industrial HDCFB, the solids level height within the storage tank should be reasonably increased to improve the driving force of the system and maintain a high solids circulation rate. When the riser height increased from 10 to 14 m, a 40% increase, the solids circulation rate decreased by 54%. When the riser height increased from 14 to 18 m, a 28% increase, the solids circulation rate decreased by 27%. It can be seen that the reduction in solids circulation rate is comparable to the riser height increase. At constant operating conditions, predicting the influence of riser height on solids circulation can aid in the design of storage tanks. In addition, the pressure drop in the cyclone separator mainly consists of friction losses, which increase significantly with higher solids circulation rates.

Fig. 5 shows the distribution contour of solids holdup in the HDCFB with different riser heights. The same driving force can be guaranteed by maintaining the same storage height. At the bottom

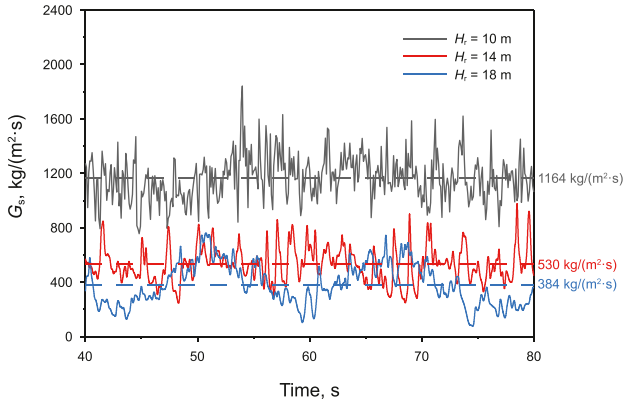

Fig. 4. Variation of solids circulation rate with time in the HDCFB of different riser heights.

of the riser, the solids holdup is high and many clusters are formed. The solids holdup in the riser decreases significantly with increasing axial height for all three HDCFBs. At the top of the riser, particles collide and accumulate on the sidewall of the elbow, leading to a region of higher solids concentration. Among the three different riser heights, the highest particle concentration occurs in the riser with a 10 m height due to the higher solids circulation rate of the 10 m high riser compared to that of the 14 m and 18 m high risers. For the HDCFB with a 10 m high riser, a large number of particles accumulate on the wall in the lower part of the cyclone separator. The particle concentration in the cyclone separator decreases significantly with increasing height of the riser due to a lower solids circulation rate. Under high-density operating of the CFB, the operational load on the cyclone separator increases significantly, which may affect separation efficiency. It is necessary to design a suitable gas-solid separation device according to the actual solids circulation rate for industrial HDCFB.

Fig. 6 shows the axial distribution of solids holdup in the risers with different heights, presented using both normalized and actual height scales. When the height of the riser increases from 10 to 18 m, the average solids holdup in the riser decreases due to the decreased solids circulation rate. Under the influence of the inlet and outlet structures, the solids holdup is higher at the bottom and top of the riser than in the middle of the riser for the three risers. In the middle of the riser, the ranges of fully developed flow differ among the risers of different heights. In the axial region from $h/H = 0.35$ to 0.75, the gas-solid flow is fully developed in the riser with 18 m height. In the axial region from $h/H = 0.4$ to 0.78, the gas-solid flow is fully developed in the 14 m riser. However, in the 10 m riser, particle fluidization is affected by the outlet structure before reaching full development, resulting in an increase in solids holdup with increasing axial height. As the solids circulation rate increases, the dimensionless height required for particles to reach the full development region also increases. For high-density operation within HDCFB, the fully developed flow is difficult to achieve in risers with low heights.

As shown in Fig. 6(b) and (c), for the riser, particle distribution in the center differs significantly from that near the wall. The solids holdup in the riser is lower at the center and higher near the wall, which is the characteristic of core-annulus flow. With increasing axial height, the particle concentration in the center of the riser gradually increases and the particle concentration near the wall gradually decreases, indicating that the radial distribution of particles inside the riser is more uniform. From the height of 10–18 m, the solids holdup near the center and wall of the riser decreases due to the decreased solids circulation rate. In the risers of 10 and 14 m in height, the solids holdup near the wall remains around 0.3, which is due to the fact that the solids holdup near the wall is saturated. This phenomenon suggests that as the solids circulation rate increases, the particle concentration near the wall is limited and the particle concentration in the center of the riser increases, which will significantly increase the gas-solid contact efficiency.

Fig. 7 shows the axial distribution of particle velocity in the risers with different heights, presented using both normalized and actual height scales. At the bottom of the riser, particles are carried by the high-velocity gas, resulting in a rapid increase in particle velocity. This region is considered the acceleration zone for the particles. The velocity difference between the gas and solid phases gradually decreases, leading to a reduction in drag force. When the drag force equals the gravitational force on the particle, the particle velocity remains constant, indicating that the gas-solid flow has reached the full development region. At the top of the riser, there is a slight increase in particle velocity, which is due to the outlet effect. A comparison of the average particle velocity shows that the variation of particle velocity in the risers with different heights is small under certain operating conditions. Combining

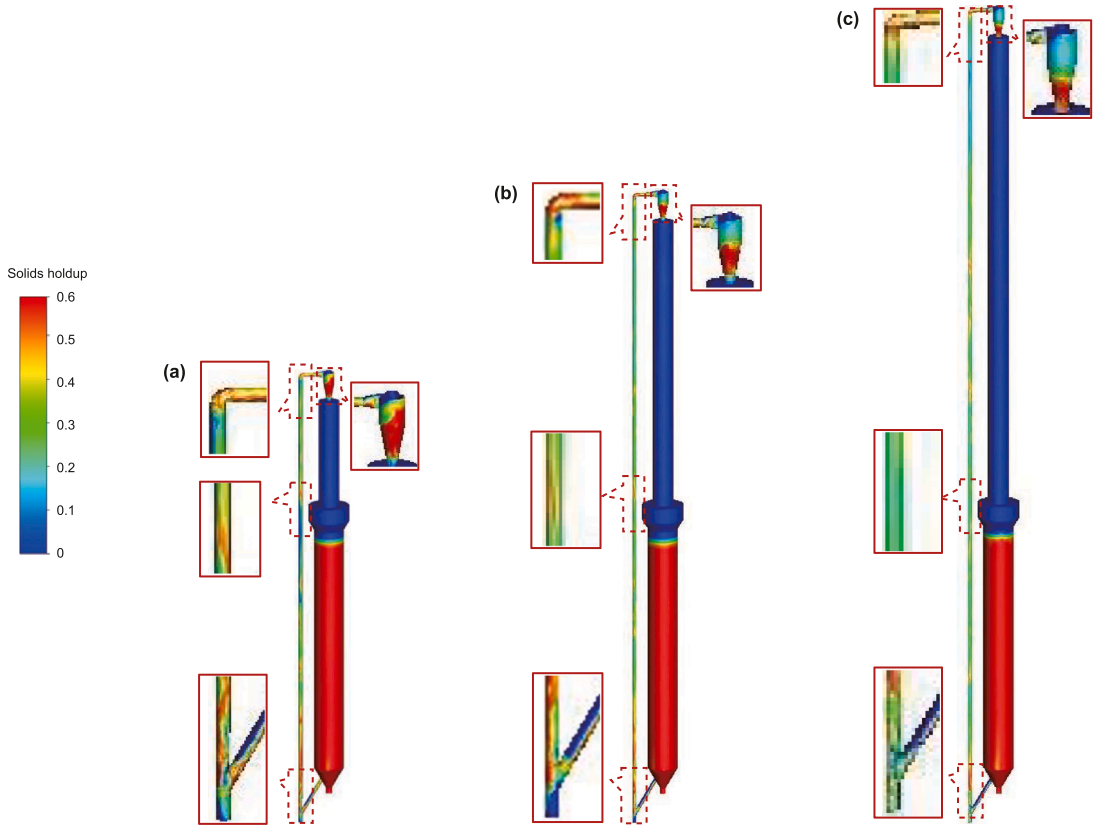

Fig. 5. Distribution contour of solids holdup in the HDCFB with different riser heights. **(a)** H_r = 10 m, **(b)** H_r = 14 m, **(c)** H_r = 18 m.

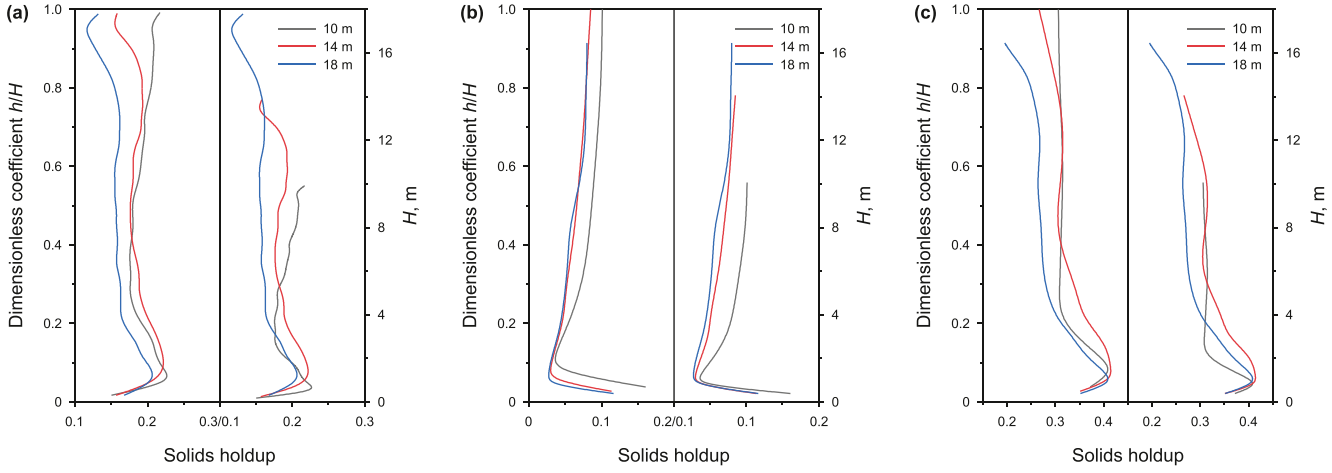

Fig. 6. Axial distribution of solids holdup in the risers with different heights. **(a)** Axial average, **(b)** center of the riser, **(c)** wall of the riser.

Figs. 6 and 7 reveals that in the middle of the riser, the average solids holdup and average particle velocity in the risers with 14 and 18 m in height are essentially constant with increasing axial height. However, the average solids holdup and average particle velocity in the 10 m riser continue to increase slowly with increasing axial height since full development has not yet been achieved. This result further suggests that for high-density operation in the HDCFB, higher height is required to enable stable gas-solid flow. Comparing the particle velocity in the center and near the wall of the risers with different heights, the particle velocities are lower in the center and higher near the wall for the risers with 10 and 14 m in height. In the 18 m high riser, the particle velocity in the center is high and the particle velocity near the wall decreases to such low magnitudes that negative values are also observed, indicating downward particle movement along the wall and subsequent particle back-mixing. This phenomenon is because particles colliding in the center of the 18 m high riser are fewer due to the lower solids holdup. At the same gas velocity, particles in the center of the riser are more easily accelerated by gas phase drag forces to the fully developed stage. Near the wall of the riser, momentum loss due to wall friction increases with increasing riser height. Therefore, the velocity near the wall of the riser with higher height is lower. Due to the core-annular flow characteristics of gas-solid fluidized beds, most particles are concentrated near

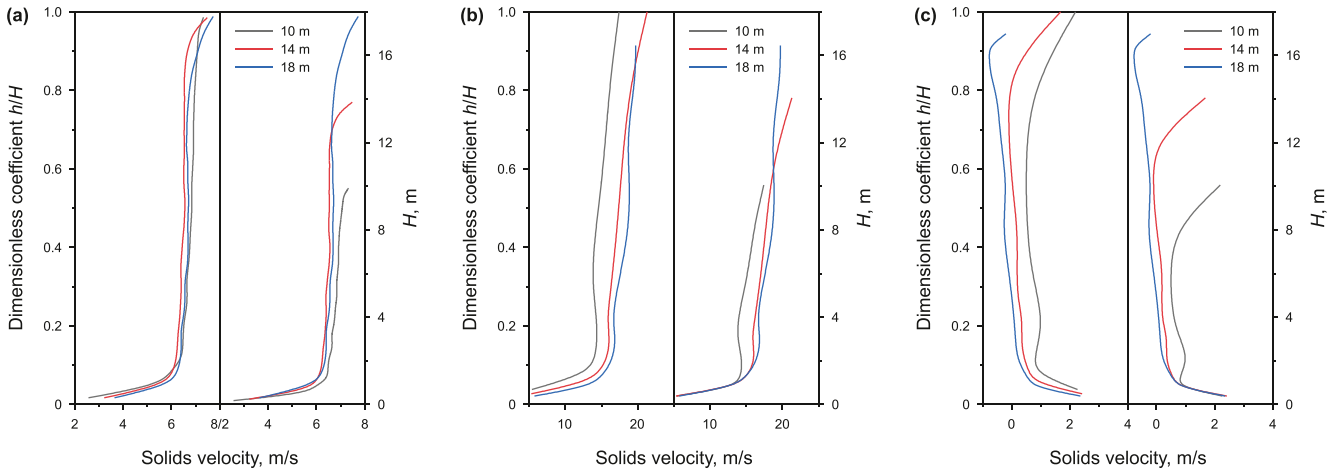

Fig. 7. Axial distribution of particle velocity in the riser with different heights. **(a)** Axial average, **(b)** center of the riser, **(c)** wall of the riser.

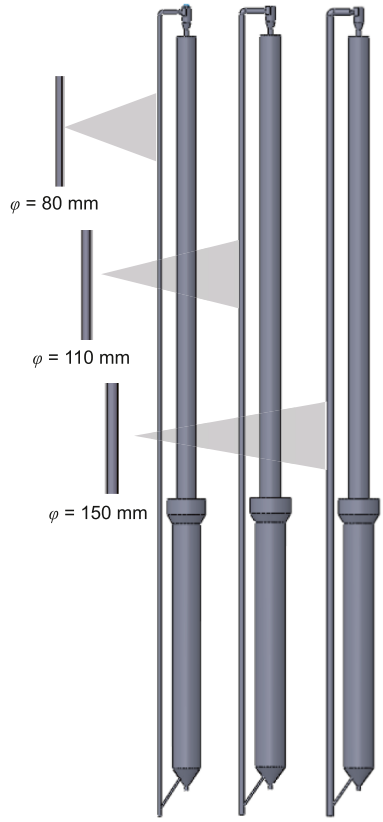

Fig. 8. Geometry of HDCFB with different riser diameters.

the reactor wall, which means that it is difficult for particles in risers with higher heights to be carried to the outlet under a given driving force and gas velocity. Therefore, for industrial-scale HDCFB with high height risers, maintaining sufficient gas mass flow rate at the bottom of the riser can improve the gas-solid drag forces and reduce particle back-mixing.

3.3. Effect of riser diameter on gas-solid hydrodynamics in the HDCFB

The diameter of the riser is below 100 mm in most experimental units, which results in significant wall effects on the overall flow field. In industrial units, the diameters of most risers are above 100 mm or even up to 1000 mm. Therefore, changes of reactor diameter can have a great influence on the radial distribution of the flow field. The flow characteristics obtained from experimental units may not fully represent the gas-solid flow behavior in industrial units. It is therefore essential to analyze the effect of riser diameter on gas-solid flow. Fig. 8 shows risers with diameters of 80, 110, and 150 mm, respectively. A storage height of 4 m was maintained to ensure suitable driving force in the HDCFB. The operating conditions were provided in Table 5.

The pressure drop in each unit of the HDCFB with different riser diameters is shown in Table 6. As the riser diameter increases, the pressure drop in each unit exhibits an approximately linear variation. The pressure drop in the riser is mainly composed of particle static pressure. With increasing riser diameter, the solids holdup in the riser decreases (Fig. 11), resulting in a lower riser pressure drop. Although the solids circulation rates in HDCFB systems with different riser diameters remain similar, the particle mass flow rate increases due to the larger cross-sectional area of the riser. In the HDCFB systems with larger riser diameters, a greater number of particles enter the cyclone separator, leading to an increased pressure drop across the cyclone due to frictional losses. The increase of particle flow in the HDCFB system reduces the volume of particles accumulated in the storage tank and feed pipe. Therefore, the pressure drop in the storage tank and feed pipe decreases with the increase of riser diameter.

Table 5
Operating conditions of HDCFB with different riser diameters.

Items	Values
Riser height, m	18
Riser diameter, mm	80, 110, 150
Superficial gas velocity, m/s	7
Storage height, m	4
Fluidized air, m^3/h	12

Table 6
Pressure distribution of HDCFB with different riser diameters.

Pressure drop, kPa	D_r = 80 mm	D_r = 110 mm	D_r = 150 mm
ΔP_{riser}	35.06	34.16	30.64
ΔP_{cyc}	0.16	0.20	0.25
ΔP_{fp}	−0.98	−0.69	−0.59
ΔP_{ds}	−34.24	−33.67	−30.30

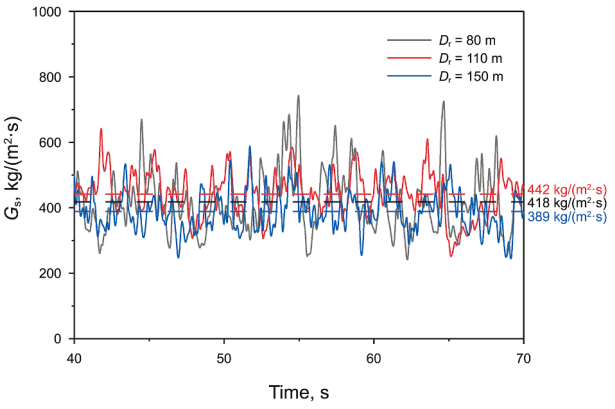

Fig. 9. Variation of solids circulation rate with time in the HDCFB with different riser diameters.

The variation in solids circulation rate over time in the HDCFB of different riser diameters remains around 400 kg/(m^2·s), as shown in Fig. 9. It can be found that the solids circulation rates of the risers with different diameters are similar, indicating that the riser diameter has less effect on solids circulation rate compared to the riser height. When the riser diameter increases from 110 to 150 mm, the solids circulation rate decreases from 442 to 389 kg/(m^2·s). This is because the gas tends to flow in the center of the reactor, and larger particle clusters form near the wall as the riser diameter increases. Larger clusters experience greater gravitational forces, making it difficult for them to be entrained into the upward flow. From the velocity distribution of the particles, it can be observed that particles near the wall in the larger-diameter risers tend to flow downward (Fig. 13), which slightly reduces the overall solids circulation rate within the system. Therefore, industrial HDCFB units with large riser diameters require higher superficial gas velocities to sustain high-density operation.

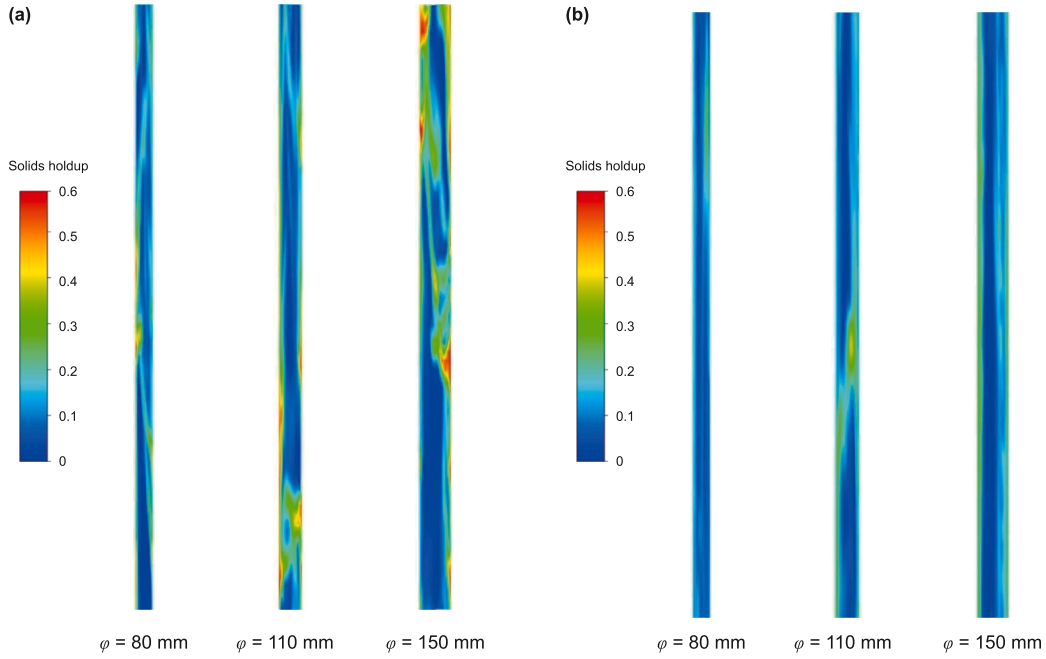

Fig. 10. Distribution contour of solids holdup in the risers with different diameters. **(a)** Bottom of the riser (2–5 m), **(b)** top of the riser (12–15 m).

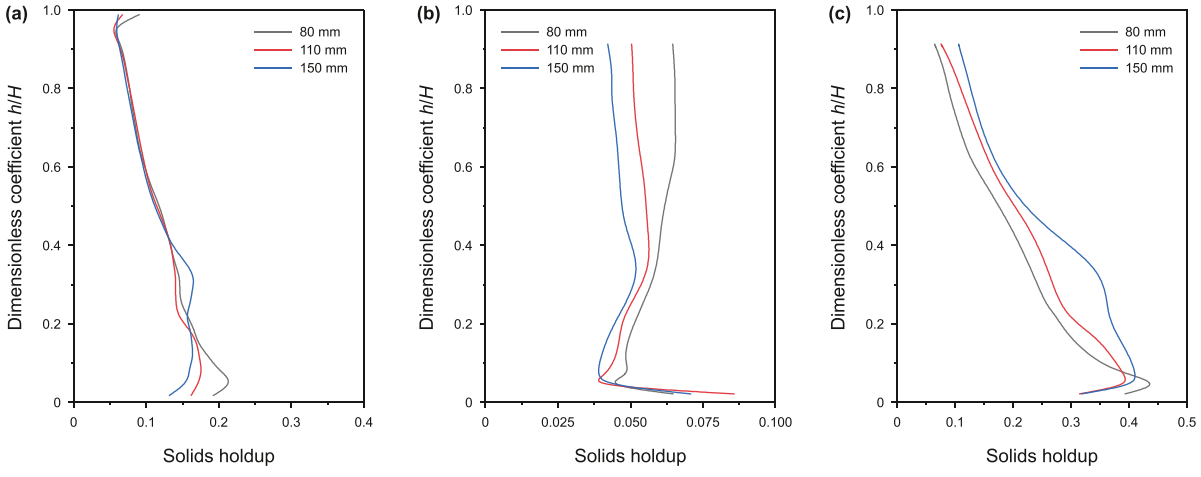

Fig. 11. Axial distribution of solids holdup in the risers with different diameters. **(a)** Axial average, **(b)** center of the riser, **(c)** wall of the riser.

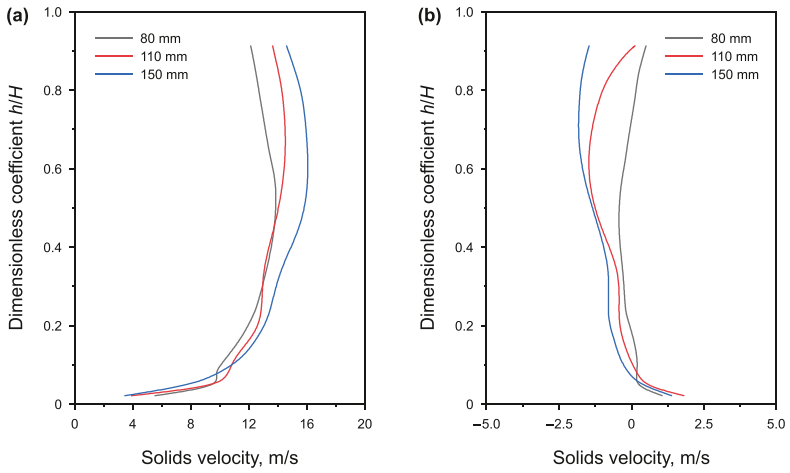

Fig. 12. Axial distribution of particle velocity in the risers with different diameters. **(a)** Center of the riser, **(b)** wall of the riser.

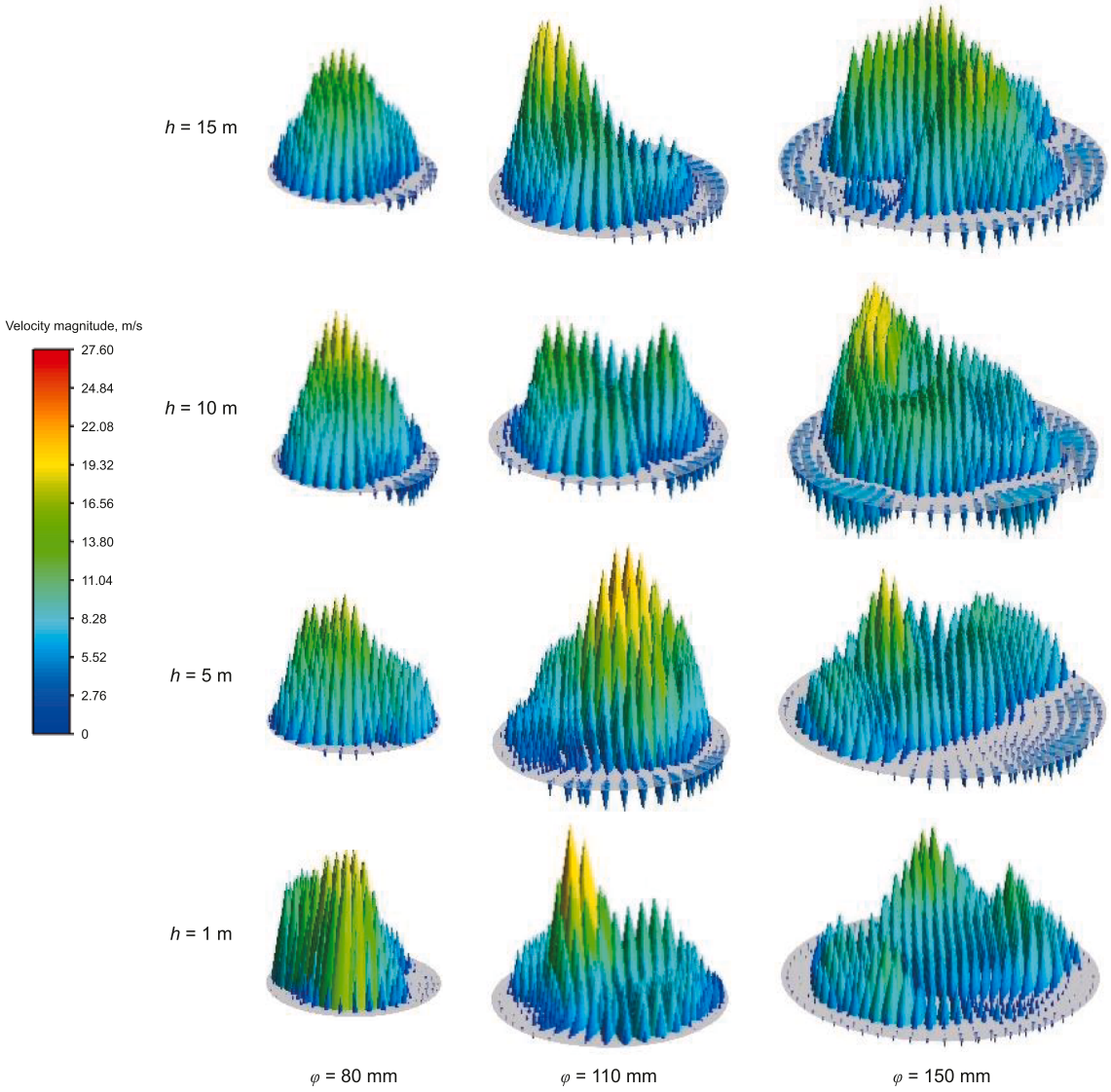

Fig. 13. Radial distribution of particle velocity vector in the risers with different diameters.

The distribution contour of solids holdup in the risers with different diameters is shown in Fig. 10. The characteristic of low solids holdup at the top of the riser and high solids holdup at the bottom of the riser can be found in all cases. At the top of the riser, the solids holdup is similar for the three risers, with lower solids holdup and clear core-annular flow characteristics. At the bottom of the riser, there are a large number of particle clusters with large sizes and different shapes. At the bottom of the riser with 80 mm diameter, some particles in the cluster move away from the core of the cluster under the influence of the upward-flowing gas, showing long tails. At the bottom of the risers with 110 and 150 mm in diameter, a large number of clusters with larger sizes are merged near the wall, resulting in complex shapes. The clusters with sizes close to the diameter of the riser are observed due to the coalescence of adjacent cluster boundaries. In the large-diameter risers, the clusters are closer to spherical in shape and have denser cores. In the reactor, the formation of a large number of clusters will reduce the gas-solid contact efficiency in the reactor and could have negative effects on heat transfer (Lv et al., 2015).

The distribution of solids holdup in the risers with different diameters is shown in Fig. 11. The difference in solids holdup at the bottom of the risers with different diameters may be due to the different degrees of particle accumulation. As the axial height increases, the average solids holdups in the risers with different diameters gradually tend to be the same. The height at which the solids holdup reaches stabilization is different for the risers with different diameters. For the risers with 80 and 110 mm in diameter, the solids holdup stabilizes above $h/H = 0.15$. For the risers with 110 mm in diameter, the solids holdup stabilizes above $h/H = 0.25$. For the risers with 150 mm in diameter, the stabilization occurs at $h/H = 0.42$. Particles in the larger-diameter riser require a longer acceleration region to reach stable flow.

Although the average solids holdups in the risers with different diameters are similar, the radial distribution of solids holdups is significantly different. As shown in Fig. 11(b) and (c), as the riser diameter increases, particles tend to aggregate near the wall, which results in a greater difference in solids holdup between the center and near the wall of the riser. This phenomenon indicates that the radial distribution of particles is less uniform as the riser diameter increases, which can lead to inefficient gas-solid contact in industrial reactors.

The axial distribution of particle velocity in the risers with different diameters is shown in Fig. 12. The figure shows the typical characteristic of high particle velocity in the center and low particle velocity near the wall. The gas in the riser tends to concentrate in the center, while particles, especially in the large-diameter riser, are driven toward the wall. The gas-solid hydrodynamics in the large-diameter riser are more complex, which takes more time and an extended acceleration region to reach stable flow. As the riser diameter increases, the particle velocity increases in the center and decreases near the wall, which means that the radial distribution of particle velocity is less uniform. It can be seen in Fig. 12(b) that the particle velocity near the wall is positive in the riser with 80 mm diameter, whereas negative values are observed in the risers with diameters of 110 and 150 mm. This result indicates downward flow of particles near the wall, as further illustrated in Fig. 13. Fig. 13 shows the radial distribution of particle velocity vectors in risers with different diameters. It can be seen that there are fewer particles flowing downward in the riser with a diameter of 110 mm, while the number of particles flowing downward in the riser with a diameter of 150 mm increases significantly, which may lead to a decrease in particle flux in the HDCFB system. When the diameter of the riser increases, the gas flows more concentrated in the center of the riser and the gas velocity near the wall is lower. The number and size of clusters near the wall increase, making it difficult for these clusters to be carried upward by the drag force from the gas phase. These observations demonstrate that severe particle back-mixing occurs in the larger-diameter riser due to inadequate gas-solid interaction. To reduce particle back-mixing and achieve a more uniform radial particle distribution in industrial HDCFB, it is critical to maintain sufficient gas mass flow rate. This optimization not only reduces accumulation of particles near the wall but also enhances overall reactor efficiency through improved gas-solid contact.

4. Conclusions

Exploring the hydrodynamics during the scale-up of the HDCFB is important for its industrial application. In this study, the Euler-Euler model was coupled with the EMMS interphase drag model and a modified solid pressure model to simulate the gas-solid flow of the full-loop HDCFB. The scale-up effects of the HDCFB were demonstrated by studying the influence of riser height and riser diameter on gas-solid flow characteristics. It was found that the riser height has a significant effect on the solids circulation rate of the CFB system and the solids holdup inside the riser, while it has little effect on the pressure drop in each unit within the system. When operating conditions are constant, the solids circulation rate and solids holdup inside the HDCFB decrease with increasing riser height. When the riser height is reduced to 10 m, the gas–solid flow has insufficient space to fully develop before reaching the outlet. As the riser height increases from 14 to 18 m, the normalized height of the fully developed gas-solid region decreases from 0.4 to 0.35 (h/H), which means that a higher riser is required to ensure complete flow development under higher solids circulation rates in the HDCFB. As the diameter of the riser increases, the solids circulation rate changes slightly, and the radial distribution of particle concentration and particle velocity becomes less uniform. As the riser diameter increases, the pressure drop inside the riser decreases and the pressure drop inside the cyclone separator increases. In larger-diameter risers, more particles tend to aggregate near the wall and form clusters with wider size distributions, which requires a longer acceleration zone to achieve a fully developed flow. When the riser diameter was increased from 80 to 150 mm, the normalized height (h/H) of the fully developed gas-solid region increased from 0.15 to 0.42. There is pronounced particle back-mixing near the wall of the larger-diameter riser due to the downward flow of clusters, which can reduce gas-solid contact efficiency. For industrial HDCFB systems, a greater driving force is required for higher-height risers to achieve high-density operation, and larger gas mass flow rates are recommended for larger-diameter risers to suppress particle back-mixing in the riser. These conclusions can provide theoretical guidance for the scale-up of HDCFB in fields such as petrochemicals, energy conversion, and environmental protection.

CRediT authorship contribution statement

Ming-Zhu Lv: Writing – review & editing, Writing – original draft, Validation, Data curation. **Yun-Peng Zhao:** Writing – review & editing, Validation, Formal analysis. **Min Wang:** Data curation. **Cheng-Xiu Wang:** Validation, Formal analysis. **Xing-Ying Lan:** Resources, Funding acquisition, Conceptualization. **Jin-Sen Gao:** Resources, Conceptualization. **Xiao-Gang Shi:** Writing – review & editing, Validation, Project administration, Conceptualization.

Declaration of interests

The authors declare that they have no known competing financial interests or personal relationships that could have appeared to influence the work reported in this paper.

Acknowledgments

The present work is financially supported by the National Key Research and Development Program (2024YFE0212400) and the National Natural Science Foundation of China (U22B20149), and hereby their supports are sincerely acknowledged.

Symbol description

ε	volume fraction
ρ	density, kg/m^3
u	velocity, m/s
p	pressure, Pa
τ	stress tensor, Pa
β	interphase momentum exchange coefficient, kg/(m^3·s)
U	two phase slip velocity, m/s
$\boldsymbol{I}$	unit tensor
γ	collisional dissipation of energy, kg/(m·s^3)
Θ	granular temperature, m^2/s^2
μ	shear viscosity, Pa·s
e_s	coefficient of restitution for particle collisions
g_0	radial distribution function
$\mu_{s,\,kin}$	dynamic viscosity, Pa·s
$\mu_{s,\,col}$	collision viscosity, Pa·s
$\mu_{s,\,fr}$	frictional viscosity, Pa·s
λ	bulk viscosity, kg/(m·s)
d_p	diameter of particle, m
κ	diffusion coefficient for granular energy, kg/(m·s)

Subscripts

m	gas phase or solid phase
g	gas phase
s	olid phase

References

Bi, H., Zhu, J.X., 1993. Static instability analysis of circulating fluidized beds and concept of high-density risers. AIChE J. 39 (8), 1272–1280. https://doi.org/10.1002/aic.690390803.

Cui, Y., Zhong, W.Q., Liu, X.J., et al., 2021. Study on scale-up characteristics in supercritical CO_2 circulating fluidized bed boiler by 3D CFD simulation. Powder Technol. 394, 103–119. https://doi.org/10.1016/j.powtec.2021.08.028.

Cui, Y., Zou, Y., Jiang, S.J., et al., 2023. Scale-up prediction of supercritical CO_2 circulating fluidized bed boiler based on adaptive PSO-SVM. Powder Technol. 419, 118328. https://doi.org/10.1016/j.powtec.2023.118328.

Dang, F.L., Wang, G., Lian, J.C., et al., 2025. Feasibility study of a process for the reduction of sulfur oxides in flue gas of fluid catalytic cracking unit using the riser reactor. Pet. Sci. 22 (2), 909–924. https://doi.org/10.1016/j.petsci.2024.09.021.

Grace, J.R., Issangya, A.S., Bai, D., et al., 2010. Situating the high-density circulating fluidized bed. AIChE J. 45 (10), 2108–2116. https://doi.org/10.1002/aic.690451009.

Guan, Y.J., Chang, J., Zhang, K., et al., 2016. Three-dimensional full loop simulation of solids circulation in an interconnected fluidized bed. Powder Technol. 289, 118–125. https://doi.org/10.1016/j.powtec.2015.11.043.

Issangya, A.S., Bai, D., Bi, H.T., et al., 1999. Suspension densities in a high-density circulating fluidized bed riser. Chem. Eng. Sci. 54 (22), 5451–5460. https://doi.org/10.1016/S0009-2509(99)00283-3.

Jin, X., Shen, Y.S., 2023. Current progress of experimental and simulation work of mixing processes in particulate systems. KONA Powder Part. J. 41. https://doi.org/10.14356/kona.2024015.

Kim, J.-S., Tachino, R., Tsutsumi, A., 2008. Effects of solids feeder and riser exit configuration on establishing high density circulating fluidized beds. Powder Technol. 187 (1), 37–45. https://doi.org/10.1016/j.powtec.2008.01.002.

Kong, B., Fox, R.O., 2017. A solution algorithm for fluid–particle flows across all flow regimes. J. Comput. Phys. 344, 575–594. https://doi.org/10.1016/j.jcp.2017.05.013.

Liu, E.B., Tang, H., Zhang, Y.H., et al., 2023. Experiment and numerical simulation of distribution law of water-based corrosion inhibitor in natural gas gathering and transportation pipeline. Pet. Sci. 20 (3), 1857–1873. https://doi.org/10.1016/j.petsci.2023.01.015.

Liu, G.D., Sun, D., Lu, H.L., et al., 2010. Computations of fluid dynamics of a 50 MWe circulating fluidized bed combustor. Ind. Eng. Chem. Res. 49 (11), 5132–5140. https://doi.org/10.1021/ie901103t.

Lu, H.L., Bie, R.S., Liu, W.T., et al., 2000. Computations of a circulating fluidized-bed boiler with wide particle size distributions. Ind. Eng. Chem. Res. 39 (9), 3212–3220. https://doi.org/10.1021/ie9808054.

Luo, K., Wu, F., Yang, S.L., et al., 2015. High-fidelity simulation of the 3-D full-loop gas-solid flow characteristics in the circulating fluidized bed. Chem. Eng. Sci. 123, 22–38. https://doi.org/10.1016/j.ces.2014.10.039.

Lv, L.Y., Lan, X.Y., Wu, Y.Y., et al., 2015. Effect of particles cluster on behavior of catalytic cracking reaction in FCC riser. CIESC J. 66 (8), 9 (in Chinese).

Nikolopoulos, A., Nikolopoulos, N., Charitos, A., et al., 2013. High-resolution 3-D full-loop simulation of a CFB carbonator cold model. Chem. Eng. Sci. 90 (10), 137–150. https://doi.org/10.1016/j.ces.2012.12.007.

Pärssinen, J., Zhu, J., 2001. Axial and radial solids distribution in a long and high-flux CFB riser. AIChE J. 47, 2197–2205. https://doi.org/10.1002/aic.690471007.

Reh, L., 1995. New and efficient high-temperature processes with circulating fluid bed reactors. Chem. Eng. Technol. 18 (2), 75–89. https://doi.org/10.1002/ceat.270180202.

Rodríguez-Machín, L., Arteaga-Pérez, L.E., Manrique, R., et al., 2023. The effect of citric acid pretreatment on composition and stability of bio-oil from sugar cane residues using a continuous lab-scale pyrolysis reactor. J. Anal. Appl. Pyrolysis 175. https://doi.org/10.1016/j.jaap.2023.106183.

Seo, M.W., Suh, Y.H., Kim, S.D., et al., 2012. Cluster and bed-to-wall heat transfer characteristics in a dual circulating fluidized bed. Ind. Eng. Chem. Res. 51 (4), 2048–2061. https://doi.org/10.1021/ie200649c.

Su, X., Wang, C.X., Lan, X.Y., et al., 2020. Flow of high solids density suspensions in an 18 m high circulating fluidized bed. Ind. Eng. Chem. Res. 59 (3), 1336–1349. https://doi.org/10.1021/acs.iecr.9b05893.

Su, X., Wang, C.X., Pei, H.J., et al., 2019. Experimental study of solids motion in an 18 m gas–solids circulating fluidized bed with high solids flux. Ind. Eng. Chem. Res. 58 (51), 23468–23480. https://doi.org/10.1021/acs.iecr.9b05462.

Tu, Q.Y., Wang, H.G., 2018. CPFD study of a full-loop three-dimensional pilot-scale circulating fluidized bed based on EMMS drag model. Powder Technol. 323, 534–547. https://doi.org/10.1016/j.powtec.2017.09.045.

Wang, C.X., Zhu, J., Barghi, S., et al., 2014a. Axial and radial development of solids holdup in a high flux/density gas–solids circulating fluidized bed. Chem. Eng. Sci. 108, 233–243. https://doi.org/10.1016/j.ces.2013.12.042.

Wang, C.X., Zhu, J., Li, C.Y., et al., 2014b. Detailed measurements of particle velocity and solids flux in a high density circulating fluidized bed riser. Chem. Eng. Sci. 114, 9–20. https://doi.org/10.1016/j.ces.2014.04.004.

Wang, M., Lan, X.Y., Wang, C.X., et al., 2021. Numerical simulation of the pilot-scale high-density circulating fluidized bed riser. Ind. Eng. Chem. Res. 60 (7), 3184–3197. https://doi.org/10.1021/acs.iecr.1c00170.

Wang, S., Luo, K., Yang, S.L., et al., 2017. Parallel LES-DEM simulation of dense flows in fluidized beds. Appl. Therm. Eng. 111, 1523–1535. https://doi.org/10.1016/j.applthermaleng.2016.07.161.

Wang, X.Y., Jiang, F., Lei, J., et al., 2011. A revised drag force model and the application for the gas-solid flow in the high-density circulating fluidized bed. Appl. Therm. Eng. 31 (14–15), 2254–2261. https://doi.org/10.1016/j.applthermaleng.2011.03.019.

Wu, Y.Y., Peng, L., Gao, J.S., et al., 2016. Numerical simulation of gas-solid bubbling bed and bubble characteristics based on EMMS drag model. CIESC J. 67 (8), 3259–3267 (in Chinese).

Wu, Y.Y., Shi, X.G., Liu, Y.C., et al., 2020. 3D CPFD simulation of gas-solids flow in the high-density downer with FCC particles. Powder Technol. 373, 384–396. https://doi.org/10.1016/j.powtec.2020.06.072.

Xiong, Q.G., Hong, K., Shu, S.L., et al., 2020. Multiscale numerical simulation of biomass thermochemical conversion: from micro to macro scales. Fuel Process. Technol. 199, 106294. https://doi.org/10.1016/j.fuproc.2019.106294.

Yan, A., Zhu, J.J., 2004. Scale-up effect of riser reactors (1): axial and radial solids concentration distribution and flow development. Ind. Eng. Chem. Res. 43 (18), 5810–5819. https://doi.org/10.1021/ie049578y.

Yan, A., Zhu, J.J.X., 2005. Scale-up effect of riser reactors: particle velocity and flow development. AIChE J. 51 (11), 2956–2964. https://doi.org/10.1002/aic.10556.

Yan, A.J., Ball, J., Zhu, J., 2005. Scale-up effect of riser reactors (3) axial and radial solids flux distribution and flow development. Chem. Eng. J. 109 (1–3), 97–106. https://doi.org/10.1016/j.cej.2005.03.017.

Yang, M., Wang, G., Han, J.N., et al., 2023. Fischer-Tropsch wax catalytic cracking for the production of low olefin and high octane number gasoline: process optimization and heat effect calculation. Pet. Sci. 20 (2), 1255–1265. https://doi.org/10.1016/j.petsci.2022.08.019.

Zhang, M.X., Yang, Z., Zhao, Y.P., et al., 2023. A hybrid safety monitoring framework for industrial FCC disengager coking rate based on FPM, CFD, and ML. Process Saf. Environ. Prot. 175, 17–33. https://doi.org/10.1016/j.psep.2023.05.004.

Zhang, N., Lu, B.N., Wang, W., et al., 2010. 3D CFD simulation of hydrodynamics of a 150 MWe circulating fluidized bed boiler. Chem. Eng. J. 162 (2), 821–828. https://doi.org/10.1016/j.cej.2010.06.033.

Zhang, Y.W., Lei, F.L., Wang, S.D., et al., 2015. A numerical study of gas-solid flow hydrodynamics in a riser under dense suspension upflow regime. Powder Technol. 280, 227–238. https://doi.org/10.1016/j.powtec.2015.04.061.

Zhao, Y.P., Shi, X.G., Wang, C.X., et al., 2023. Study on flow characteristics of turbulent fluidized bed with variable gas velocity due to chemical reactions. Powder Technol. 416, 118211. https://doi.org/10.1016/j.powtec.2022.118211.

Zheng, Z.H., Ma, J.N., Yan, Z.H., et al., 2025. Pressure characterization study in the jet influence zone of riser based on HHT analysis. Pet. Sci. 22 (7), 3056–3067. https://doi.org/10.1016/j.petsci.2025.04.015.

Zhong, H.B., Sun, Z.N., Zhu, J., et al., 2021. Prediction of solid holdup in a gas–solid circulating fluidized bed riser by artificial neural networks. Ind. Eng. Chem. Res. 60 (8), 3452–3462. https://doi.org/10.1021/acs.iecr.0c05474.